Fusion Engineering and Design 175 (2022) 112991

Contents lists available at ScienceDirect

Fusion Engineering and Design

journal homepage: www.elsevier.com/locate/fusengdes

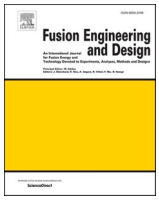

Design of a multi-isotopic hydrogen co- and counter-permeation experiment for HCPB related tritium mitigation studies

S.J. Hendricks *, E. Carella, D. Jimenez, J.M. Garcia, J. Molla

Ciemat, Av. Complutense, 40, 28040 Madrid, Spain

ARTICLE INFO

Keywords:
HCPB
Tritium mitigation
Multi-isotopic transport
Co-permeation
Counter-permeation
Permeation experiment

ABSTRACT

A safe operation of the HCPB breeding blanket requires tritium permeation from the breeder into the coolant to be kept as low as possible. Previous studies could identify co- and counter-permeation of different hydrogen isotopes as a method to affect the permeation fluxes of the involved species. For the investigation of multi-isotopic transport as a permeation mitigation or enhancement mechanism in an HCPB related environment a new permeation experiment has been designed in which tritium is substituted by deuterium. It consists of two gas cavities inside of a vacuum chamber separated by a EUROFER sample disk that can be heated to temperatures of up to 600 °C. The set-up allows injecting arbitrary partial pressure combinations of H_2 and D_2 into each chamber. Co- and counter-permeation processes can be analysed for different temperatures and pressure configurations by measuring the occurring deuterium permeation fluxes using a calibrated quadrupole mass spectrometer. Apart from the determination of characteristic hydrogen isotope transport coefficients of the sample material the presented experiment is designed to serve as a validation tool for existing multi-isotopic transport models which are used to explain and simulate co- and counter-permeation effects in breeding blankets.

1. Introduction

Enabling tritium self-sufficiency of future fusion reactors is one of the main purposes of the breeding blanket system (BB). Amongst others, the helium cooled pebble bed (HCPB) is a solid breeding blanket concept currently under development [1,2]. In this BB design lithium containing ceramic pebbles (Li_4SiO_4, Li_2TiO_3 compositions [3]) are densely packed and stored in compartments surrounding the plasma facing first wall. They are separated by beryllium layers serving as neutron multipliers. Nuclear reactions between high-energy neutrons coming from the fusion plasma and the lithium result in a generation of tritium which diffuses to the ceramic pebble surfaces. The interstitial sites of the pebble bed are rinsed by a He + H_2 purge gas. By adding H_2 to the purge gas recombination and isotope exchange reactions occur causing the release of HT, T_2, H_2O, HTO and T_2O into the gas [4–7]. The purge gas carries the liberated tritiated molecules to a tritium extraction system [8].

The heat produced by the neutron multiplying and tritium breeding reactions is absorbed by the purge gas and transferred through EUROFER channel walls into a helium coolant where pressurized helium gas acts as the coolant fluid. Due to the relatively high hydrogen isotope permeability of EUROFER [9] a significant fraction of the H_2, T_2, HT, H_2O, HTO and T_2O molecules will dissociate and dissolve into the channel walls causing a diffusive transport of protium and tritium through the metal bulk before they recombine and enter the coolant. Although the HCPB concept exhibits the least severe level of coolant contamination among all BB designs, for a safe operation it is essential to minimize the permeation flux of tritium from the purge gas into the coolant as much as possible. For this purpose different methods have been proposed and are currently under intense investigation. One technique focuses on the application of tritium permeation barrier materials coated on the interior wall of the purge gas channels [10]. Another approach consists in a controlled injection of H_2 gas into the coolant which leads to a simultaneous co- and counter-permeation of protium and tritium from both sides through the EUROFER channel

Abbreviations: BB, Breeding blanket; COOPER, Co- and counter-permeation experiment; CL, Calibrated leak; DAI, Data acquisition interface; GMT, Gas mixing tank; H, Heater; HCPB, Helium cooled pebble bed; HTR, Heat transfer ring; LP, Leak path; LV, Leak valve; OC, Outer chamber; OP, Open path; PFD, Process flow diagram; PSU, Power supply unit; PC, Permeation cell; PG, Pressure gauge; PT, Permeation tube; QMS, Quadrupole mass spectrometer; RVP, Rotary vane pump; SD, Sample disk; TC, Thermocouple; TMP, Turbo molecular pump; V, Valve.

* Corresponding author.
E-mail address: sebastian.hendricks@ciemat.es (S.J. Hendricks).

https://doi.org/10.1016/j.fusengdes.2021.112991
Received 9 August 2021; Received in revised form 19 November 2021; Accepted 17 December 2021
Available online 2 January 2022

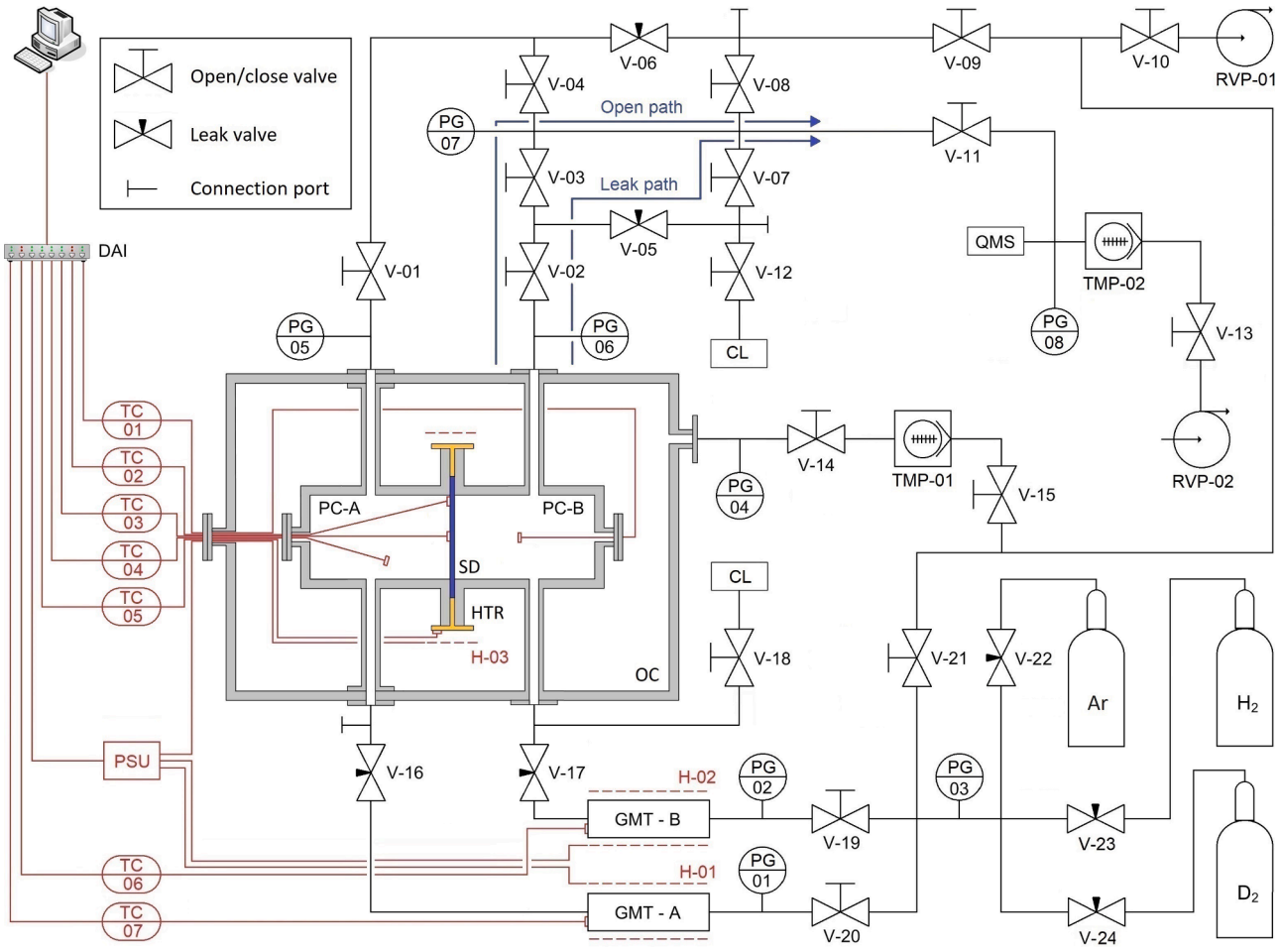

Fig. 1. Process flow diagram of the COOPER experimental set-up (CL: Calibrated leak, DAI: Data acquisition interface, GMT: Gas mixing tank, H: Heater, HTR: Heat transfer ring, OC: Outer chamber, PC: Permeation cell, PG: Pressure gauge, PSU: Power supply unit, QMS: Quadrupole mass spectrometer, RVP: Rotary vane pump, SD: Sample disk, TC: Thermocouple, TMP: Turbo molecular pump, V: Valve).

walls. Previous experiments and numerical models suggest that in certain H_2 partial pressure regimes this could have a mitigating or enhancing effect on the net amount of permeating tritium into the coolant [11–21]. For a detailed experimental investigation of this phenomenon a new multi-isotopic **CO**- and c**O**unter-**PER**meation experiment (COOPER) has been designed within the scope of this work. The experiment enables quantitative permeation flux measurements of H_2, D_2 and HD from a gas chamber through a thin EUROFER disk into a second gas chamber. Both chambers can be filled with an arbitrary partial pressure distribution of D_2 and H_2 gas. Thus, co- and counter-permeation scenarios under HCPB conditions are experimentally recreated using D_2 gas instead of tritium containing molecules. The aim is to study the effect different H_2 partial pressure proportions in the two chambers have on the net flux of permeating deuterium atoms. In contrast to similar previous experimental devices the hot permeation cells of the COOPER experimental set-up are mounted inside of a vacuum chamber. In this way, leakages or permeation of atmospheric gases into the interior of the gas chambers can be drastically reduced. Moreover, the vacuum will guarantee an efficient degassing of the permeation cells after each measurement procedure. This provides a cleaner permeation environment and helps eliminating difficult to estimate uncertainty factors of the measurement results. A further objective of the COOPER experiment is the validation of a developed numerical simulation tool [17,19,20] which allows calculating multi-isotopic transport in the HCPB breeding blanket system. In addition, the COOPER experiment enables experimentally determining general hydrogen transport parameters like the permeability, the diffusivity as well as surface rate constants of hydrogen isotopes in the sample disk material. The design and operation principle of the COOPER experiment as well as preliminary measurement procedures are presented in this article.

2. Experimental design

The process flow diagram (PFD) of the entire experimental set-up can be seen in Fig. 1. A cubic shaped vacuum chamber made of 316 stainless steel forms the centrepiece of the experiment. It is called outer chamber (OC). A photo of the fabricated outer chamber is shown in Fig. 2.

The front and back plane of the OC are open and form flanges with embedded Viton gaskets. They are closed by cuboid shaped cover plates. One cover plate provides a connection to electrical and thermocouple feedthroughs. At the roof of the OC there is another access to the OC which is linked to a turbo molecular pump (TMP-01) with a maximum pumping speed of $S_{\mathrm{TMP-01}} = 0.2\mathrm{m}^3/\mathrm{s}$ as well as to a rotary vane pump (RVP-01). In the molecular flow regime the conductance of the pipe connecting the OC and the TMP-01 is estimated to be of the order of $C_{\mathrm{OC}} \approx 15 \times 10^{-3}\mathrm{m}^3/\mathrm{s}$. Preliminary vacuum and degassing tests could confirm that the interior of the OC is successfully maintained at vacuum pressures of about 1×10^{-4}Pa which is controlled by a wide range pressure transmitter PG-04.

The OC houses the permeation cells A and B (PC-A and PC-B), which is where the investigated permeation processes take place. A photo of the PCs mounted inside of the OC is presented in Fig. 3. It shows PC-A in

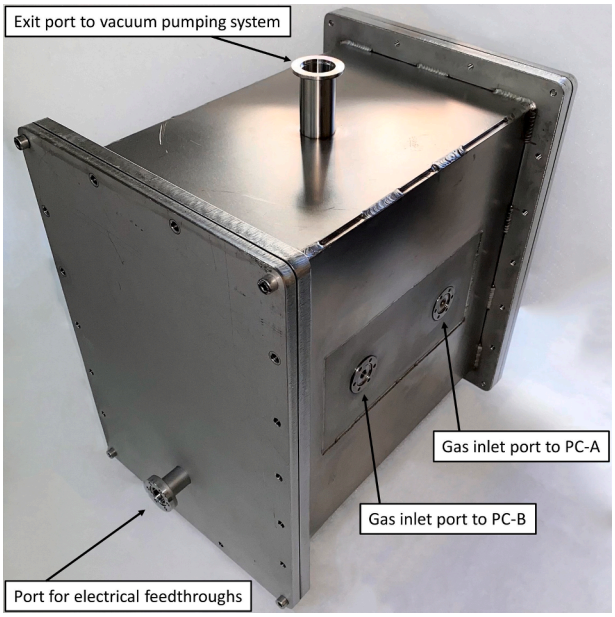

Fig. 2. Photo of the fabricated co- and counter-permeation chamber separated from the rest of the experimental system. The picture shows the outer vacuum chamber which hosts the permeation cells A and B. The two gas outlet ports sit on the rear side of the chamber, opposite to the visible gas inlet ports.

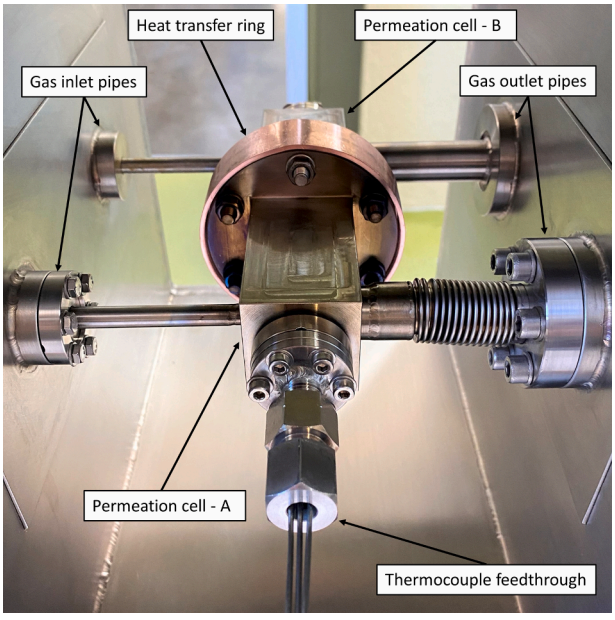

Fig. 3. Photo of the permeation cells A and B mounted inside of the outer chamber.

the front connected to PC-B which is visible in the back. A section cut of the permeation cell system can be seen in Fig. 4.

Both PCs consist of identical square shaped thick walled 316 stainless steel chambers with cylindrical inner cavities. Their flat back walls are welded to mini ConFlat flanges which are connected to high temperature graphite sealed thermocouple feedthroughs. As visible in the centre of Fig. 4 each PC ends in a wide open flange which enables a screwed connection of the two chambers. Gas can enter and exit each PC through a narrow gas inlet pipe and a wider outlet pipe. The two inlet ports and two outlet ports penetrate the vertical walls of the OC at opposite sides (see Fig. 2 and 3). While the inlet and outlet pipes of PC-B are welded from inside against the OC walls, the pipes of PC-A exhibit a screwed connection via interior ConFlat flanges. This design allows completely detaching and removing PC-A from the system while PC-B will always remain in its fix position. In this way the possibility of leakages at the flange connections is reduced. Placing the copper gaskets and tightening the screws of the ConFlat flanges of PC-A requires some longitudinal and transversal clearance of at least one of the gas pipes. Therefore, the gas outlet pipe of PC-A consists of a flexible bellow tube. Outside of the OC the inlet and outlet ports terminate in welded ConFlat flanges.

The COOPER experiment is designed to enable permeation measurements of $i = \{H_2, D_2, HD\}$ gas through a $d_{SD} = 1$mm thick round sample disk (SD) which is clamped between the two inner custom made flanges of the PCs using high temperature screws made of Incoloy® A-286. Special focus is placed on EUROFER as the disk material. For accurate measurements very good leak tightness between the PCs and the SD is essential. Due to high disk temperatures of up to 600 °C it is chosen to use custom designed Helicoflex® O-rings for the sealing which are made of a silver plated Inconel® 600 jacked surrounding an internal Nimonic® 90 spring. The effective circular disk surface which is in contact with the interior gas of each PC has has a value of approximately $A_{SD} = 9.1 \times 10^{-4}\text{m}^2$.

The position of the gaskets in contact with the SD is highlighted in Fig. 5. It shows the assembly steps of the permeation system. In order to heat up the sample disk to the mentioned temperature regime a cylindrical band heater (H-03) is used. It is clamped around a copper cylinder which is called heat transfer ring (HTR). It can be seen in the lower left image of Fig. 5. On its inner surface the HTR merges into a flat copper disk with a circular cut-out in its centre. The SD is placed inside of the cut-out. Tightening the clamping screw of the band heater increases the contact force between HTR and SD which leads to a good thermal contact. As soon as the band heater is switched on, heat quickly diffuses into the HTR disk sitting between the PCs before it enters the SD. Since the HTR is in tight contact with the PC flanges, they will heat up too. The heat enters the SD through the contact surface between the HTR and the SD as well as through the contact surface between the PC flanges and the SD. This custom-designed external heating system prevents an outgassing of impurities from the heater into the measurement system during operation. Instead, molecules that evaporate from the PCs or the heater into the OC will be quickly removed by the TMP-01. In this way, an efficient degassing of any residual protium, deuterium or atmospheric molecules from the PC walls into the vacuum system is guaranteed. This is an important requirement for accurate permeation measurements. The system consisting of the permeation cells, the heat transfer ring and the sample disk will be called permeation tube (PT). The fact that the PT sits inside of the vacuum chamber ensures the presence of a very clean environment in which the permeation and leakage of atmospheric gases from outside the PT into the interior of the hot PCs is highly reduced. To estimate the temperature profile that would establish in thermal equilibrium inside of each component a 3D model of the PT together with the OC is imported into the finite element software ANSYS using the steady-state thermal analysis tool. It is assumed that the contact surface of band heater and HTR is maintained at a constant temperature of 650 °C. For the inner walls of the evacuated OC and the surfaces of the PT only heat transfer by thermal radiation and thermal contact conductance are taken into account while outside of the OC also heat transfer through air convection is considered. It is found that in thermal equilibrium the PC walls would be in average 150 °C - 220 °C colder than the HTR. As in other permeation experiments [22] it is to expect that a fraction of the induced hydrogen isotope gas will escape by permeation through the PC walls. Since the PCs are located in a vacuum chamber and not in air the transport of hydrogen isotopes through the metal walls into the OC can be accurately simulated using well known hydrogen transport parameters of 316 stainless steel. Therefore, a numerical model of the COOPER experiment is currently under development. It will allow theoretically quantifying the mentioned permeation losses for each measurement so that it can be

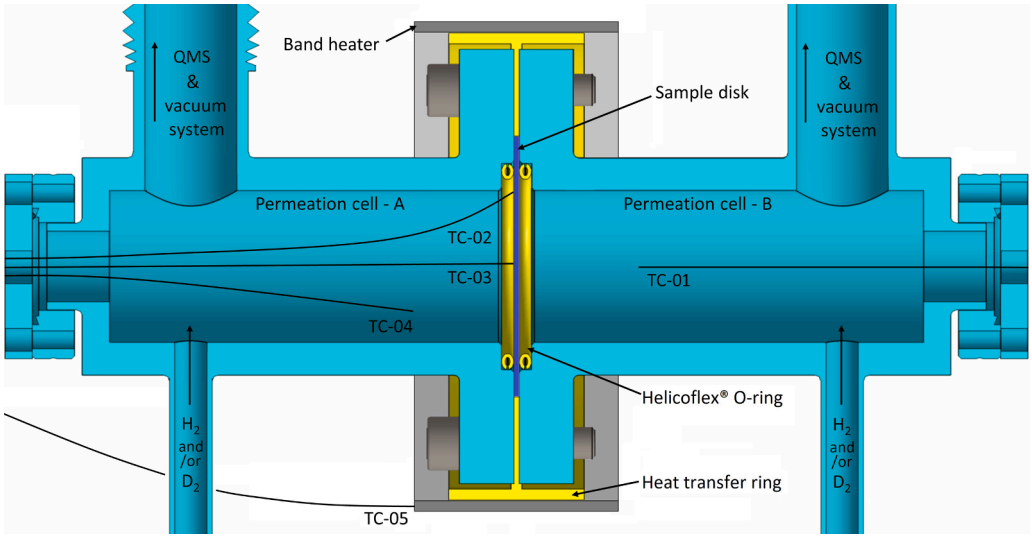

Fig. 4. Section cut of the inner permeation cells which are separated by the sample disk and a heat transfer copper ring.

considered in the evaluation of the experimental results. The calculated temperature profile in thermal equilibrium which establishes throughout the HTR attached to the SD is presented in Fig. 6. It shows that the temperature of the copper ring would decrease from 650 °C at the HTR jacket to 607 °C at the contact surface of HTR and SD. Thermocouple TC-02 which is attached to the SD close to the Helicoflex gasket would indicate a temperature of about 595 °C. Thermocouple TC-03 which sits in the centre of the SD would measure a value of approximately 587 °C. Hence, the simulation indicates that the designed heating system would lead to a very small radial temperature gradient in the SD of only about $\Delta T = 10\,^{\circ}\mathrm{C}$. Ensuring a flat radial temperature profile of the sample disk is essential for meaningful and precise experimental results. The band heater is fed by a direct current power supply unit (PSU) which is linked to an electrical feedthrough attached to the exit flange at the cover plate of the OC. Thermocouple TC-05 measures the temperature of the interior heating zone of the band heater. The temperature data provided by all thermocouples is read out by a computer. The connection is established by a data acquisition interface (DAI). A LabVIEW program uses the temperature data measured by thermocouple TC-05 to control the heating power. In this way the SD can be heated with an arbitrary temperature ramp before it reaches the desired stationary state temperature.

The two exterior ConFlat flanges linked to the inlet gas pipes of the PT are connected to a gas line system (see Fig. 1). The system permits inserting an arbitrary partial pressure configuration of H_2 and D_2 into each PC via all-metal leak valves (V-16 and V-17) which are attached to the gas inlet ports. Adjustable gas flows in a range $1 \times 10^{-10}\,\mathrm{mbarl\,s^{-1}}$ - $500\,\mathrm{mbarl\,s^{-1}}$ enable a controlled injection of gas pressures between 1×10^{-1}Pa and 1×10^{5}Pa. The gas temperatures inside of PC-A and PC-B are measured by the thermocouples TC-01 and TC-04. Via flexible stainless steel tubes both gas inlet valves are linked to custom-made gas mixing tanks (GMT-A and GMT-B) with a volume of about 100ml , each. A photo of the gas line system detached from the gas bottles is shown in Fig. 7. The GMTs serve as gas reservoirs where the different gases used in the experiment can be mixed with an arbitrary partial pressure configuration and pre-heated before being injected into the PCs. Therefore, both GMTs are wrapped with heating cables (H-01 and H-02) and isolated by thermal insulation superwool® fibre. Pre-heating the gas before it enters the PCs avoids an abrupt cooling of the hot sample disk in the moment of the gas injection. Like the band heater the heating cables of the GMTs are controlled by a LabVIEW based control program which uses temperature measurement data from two installed thermocouples (TC-06 and TC-07) as input parameters. The gas pressure inside of each of the two tanks is controlled by a capacitance diaphragm pressure gauge (PG-01 and PG-02) with a measurement range of 1.3×10^{1}Pa - 1.3×10^{5}Pa. Two bellow sealed high temperature valves (V-19 and V-20) are placed right behind the pressure sensors and serve as open-close gates for the GMTs. Both valves are linked to a gas line intersection which exhibits a connection to an Ar, H_2 and D_2 gas cylinder. Each of them is equipped with a pressure regulator and a fine flow needle valve (V-22, V-23 and V-24). The intersection has a further connection to the RVP-01 via valve V-21 and a Pirani pressure transmitter PG-03. Following an initial evacuation of the entire gas line system both GMTs can be successively filled with individual gas mixes of arbitrary partial pressure compositions. The argon gas is used to vent the tube system whenever it is required and provides the possibility to create gas mixes of Ar and H_2 and/or D_2 in the GMTs. In this way, H_2 and D_2 partial pressures of even below 1×10^{-1}Pa can be injected and maintained stable inside of the PCs.

To insert a gas mix into GMT-A the needle valve belonging to the first gas component is carefully opened until the desired partial pressure fraction is reached. Then, the needle valve of the next gas component is manipulated until the aimed partial pressure composition of the second gas component is attained. The partial pressure of the second gas is equal to the momentary pressure subtracted by the final pressure after the previous gas was filled in. If a third gas component is added to the mix this process is repeated. As soon as GMT-A contains the right gas composition, valve V-20 is closed and the gas line intersection is evacuated. To fill GMT-B valve V-19 is opened and the gas filling procedure is repeated introducing a new arbitrary partial pressure composition. The prepared gas mixes are injected into the PCs after the sample disk has reached its desired temperature using the leak valves V-16 and V-17.

The two exit ports of the outlet gas pipes of the OC are each connected to two capacitance diaphragm pressure gauges, one for a measurement range between 1.3×10^{-1}Pa - 1.3×10^{3}Pa and one with a range of 1.3×10^{1}Pa - 1.3×10^{5}Pa. The two pressure gauges of PC-A share the name PG-05 while the tow gauges connected to PC-B are associated with the label PG-06. By opening V-01 and accordingly V-02 both PCs exhibit a connection to a HAL 101X RC quadrupole mass spectrometer (QMS) from Hiden Analytical and a turbo molecular pump (TMP-02) whose exhaust is linked to a separate rotary vane pump (RVP-02). The TMP-02 has a maximum pumping speed of about $S_{\mathrm{TMP-02}} = 0.2\mathrm{m}^3/\mathrm{s}$. During a permeation measurement the tube line of only one of the PCs is opened to the measurement and vacuum system at a time. This depends on whether the permeation flux from PC-A to PC-B (defined as permeation direction AB) or from PC-B to PC-A (defined as

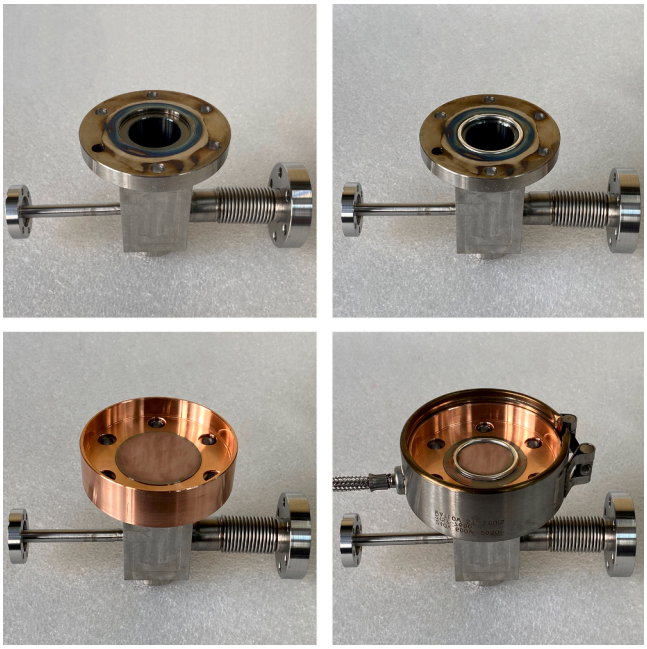

Fig. 5. Photos showing the assembly steps of the permeation tube. **[upper left]** Open flange of the detached PC-A. **[upper right]** A Helicoflex® O-ring is placed in the prepared gasket bed of PC-A. **[lower left]** A heat transfer copper ring is centred on top of the open flange. The sample disk is placed in the round cut-out of the copper ring sitting on top of the Helicoflex® O-ring. **[lower right]** A second Helicoflex® gasket is centred on top of the sample disk. To insert heat into the sample disk a band heater is clamped around the cylinder jacket of the heat transfer ring. The shown system will be linked to the flange of PC-B.

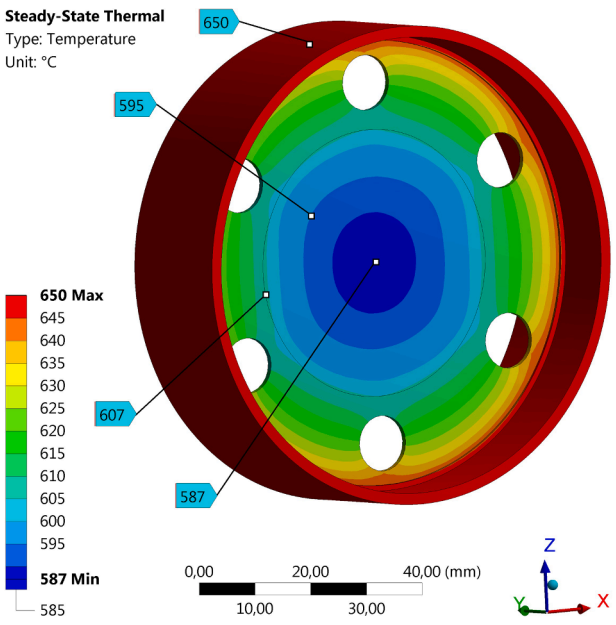

Fig. 6. Temperature profile in thermal equilibrium establishing throughout the heat transfer ring attached to an EUROFER sample disk sitting in its centre.

permeation direction BA) is measured. Both PCs are linked to the measurement system via two distinct paths. The *open path* (OP) is defined as a way through the tube system via an open-close bellow sealed valve (AB: V-03, BA: V-04). The conductance of this connection is calculated to be of the order of $C_{\mathrm{OP}} \approx 1 \times 10^{-3}\mathrm{m}^3/\mathrm{s}$. In contrast, the *leak path*

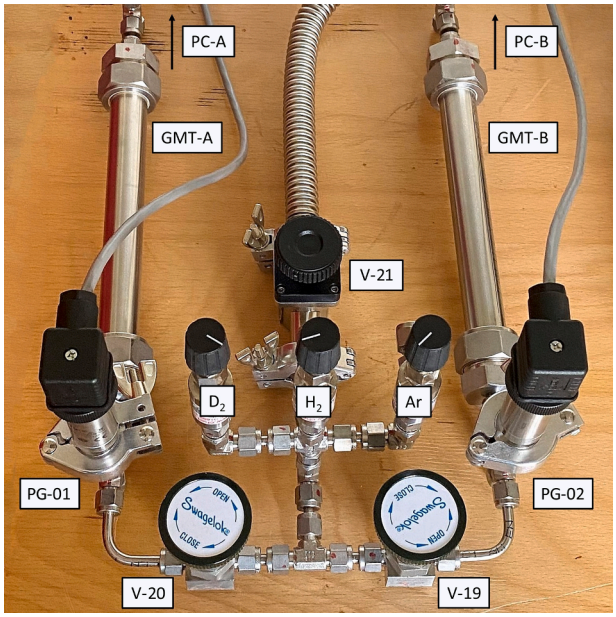

Fig. 7. Photo of the gas line system without heating wires and thermal insulation.

describes a way through the tubes which is interrupted by a leak valve (AB: V-05, BA: V-06). This allows controlling the gas leak rate from the downstream PC (AB: PC-B, BA: PC-A) to the measurement system in a range between $1 \times 10^{-10}\mathrm{mbar}l\mathrm{s}^{-1}$ and $500\mathrm{mbar}l\mathrm{s}^{-1}$. The enclosed gas volume reaching from the SD up to the leak valve is determined using a CAD model of the set-up with which we obtain $V_{\mathrm{LP}} \approx 764 \pm 5 \times 10^{-6}\mathrm{m}^3$. The conductance of the pipe system linking the corresponding leak valve with the QMS is calculated to be of the order of $C_{\mathrm{LP}} \approx 1 \times 10^{-3}\mathrm{m}^3/\mathrm{s}$. Continuous total gas pressure measurements in the pipe system are performed by the wide range pressure transmitters PG-07 and PG-08 (see Fig. 1).

2.1. Measurement of D permeation flux into vacuum

For permeation flux measurements from a gas filled PC into vacuum the evacuated PC and the QMS are linked via the *open path*. Preliminary vacuum measurements confirmed that the vacuum system permits evacuating the *open path* to minimum pressures of about 5×10^{-6}Pa at the QMS (measured by PG-08) and about 1×10^{-5}Pa closer to the PCs (measured by measured by PG-07). At higher temperatures maintaining these pressure levels requires previous degassing operations. The QMS enables simultaneous partial pressure measurements of different gas molecules over a wide molecular mass range. This includes the molecules H_2 (2 amu), HD (3 amu) and D_2 (4 amu). Although D_2 and He occupy the same atomic masses they exhibit different ionisation energies. The utilized QMS inherits an operation mode which allows complete control over the electron energy inside of its ionisation source known as threshold ionisation mass spectrometry [23]. It enables a differentiation of the mentioned interfering molecules. Since for the used QMS the gas specific relative sensitivities and fragmentation patterns are known the conversion of the detected ion currents into a partial pressure becomes possible. The QMS enables permeation flux measurements through the sample disk by measuring the partial pressure increment $\Delta P_i(t) = P_i(t) - P_{0,i}$ of molecule i in the *open path* of the downstream PC as it has been done in previous experiments [11–13]. Here, $P_{0,i}$ stands for the base partial pressure of molecule i that establishes before the D_2 gas is injected while $P_i(t)$ describes the measured partial pressure during deuterium permeation. To convert the detected pressure increment into a permeation flux we use [13]:

$$J_{\mathrm{perm},i}(t) = \frac{\Delta P_i(t)\cdot S_{\mathrm{eff,OP},i}}{RTA_{\mathrm{SD}}} \tag{1}$$

The pressure increment that establishes at a certain permeation flux depends on the effective pumping speed of the *open path* $S_{\mathrm{eff,OP},i}$ which slightly varies for different molecular species i [24]. Since $C_{\mathrm{OP}} \ll S_{\mathrm{TMP-02}}$ it is to expect that $S_{\mathrm{eff,OP},i} \approx C_{\mathrm{OP}}$. For permeation to vacuum measurements the values of $S_{\mathrm{eff,OP},i}$ can be experimentally determined using calibrated H_2 and D_2 leaks (CL) of known leak rate $\dot{n}_{\mathrm{CL},i}$. Therefore, the corresponding CL is connected to the desired gas inlet port via valve V-18. The pressure increment ΔP_i registered by the QMS which results from the known particle flux of the CL of molecule i will provide $S_{\mathrm{eff,OP},i}$ by applying the expression:

$$S_{\mathrm{eff,OP},i} = \frac{\dot{n}_{\mathrm{CL},i}RT}{\Delta P_i} \tag{2}$$

Since no calibrated HD leaks exist on the market the pumping speed for HD can be estimated through $S_{\mathrm{eff,HD}} \approx 1/2\cdot(S_{\mathrm{eff,H_2}} + S_{\mathrm{eff,D_2}})$. Before the base pressure is measured and the CL is exposed to the vacuum of the *open path*, the SD is heated to the final operation temperature. In this way, leakages and permeation losses are taken into account as they would occur during a permeation flux measurement.

2.2. Measurement of D permeation flux into H_2 filled chamber

To measure the permeation flux into a gas filled PC the valves V-03 and V-04 are kept closed and the *leak path* over the respective leak valve is chosen. This requires opening valve V-07 in case of AB or valve V-08 in case of BA. The *leak path* enables maintaining the pressure in the downstream PC in the lower vacuum regime while the space surrounding the QMS is evacuated by the TMP-02 reaching the high vacuum regime of $P < 1 \times 10^{-2}$Pa where QMS measurements become possible. To do so, a sufficiently small gas leak rate through the gas leak valve needs to be adjusted. Hence, in contrast to previous counter-permeation experiments the QMS is exposed to a much lower H_2 pressure [12]. For this reason, it is to expect that the generation H_3^+ ions in the QMS ionizer is low and that an interference with the detection of HD^+ ions is rather unlikely. The total gas pressure $P_{\mathrm{tot,PC}}$ in the downstream PC is continuously monitored with the corresponding capacitance pressure gauges (AB: PG-06, BA: PG-05). The leak rate $\dot{n}_{\mathrm{LV},i}$ of molecule i through the leak valve is determined with the QMS. Therefore, the partial pressure increment $\Delta P_{\mathrm{QMS},i}$ is measured which occurs when opening the leak valve to the desired leak rate. For the leak rate of molecule i through the leak valve we find:

$$\dot{n}_{\mathrm{LV},i} = \frac{\Delta P_{\mathrm{QMS},i}\cdot S_{\mathrm{eff,LP},i}}{RT} \tag{3}$$

In the Eqs. (1)–(3) the variable T labels the gas temperature inside of the QMS which is considered to be room temperature. To measure the effective pumping speeds $S_{\mathrm{eff,LP},i}$ of the path connecting the leak valve with the QMS the calibrated leaks of the different molecules are now connected via valve V-12 right behind the leak valve of the leak path. Their values are experimentally obtained in the same manner as described in Section 2.1 by applying Eq. (2). The measurement of the permeation flux of molecule i into the downstream permeation cell is based on the assumption that:

$$J_{\mathrm{perm},i}(t) = \frac{\dot{P}_{\mathrm{PC},i}(t)\cdot V_{\mathrm{LP}}}{RT_{\mathrm{gas,PC}}A_{\mathrm{SD}}} + \frac{\dot{n}_{\mathrm{LV},i}}{A_{\mathrm{SD}}} \tag{4}$$

In this expression $\dot{P}_{\mathrm{PC},i}(t)$ is the time derivative of the partial pressure of molecule i inside the gas filled downstream PC. It can be determined from the measured leak rates assuming that:

$$P_{\mathrm{PC},i}(t) \approx P_{\mathrm{PC,tot}}(t)\cdot\frac{\dot{n}_{\mathrm{LV},i}}{\sum_i \dot{n}_{\mathrm{LV},i}} \tag{5}$$

The temperature $T_{\mathrm{gas,PC}}$ in Eq. (4) refers to the average gas temperature in the downstream PC. For atomic deuterium permeation flux measurements we define:

$$J_{\mathrm{perm,D}} = 2J_{\mathrm{perm,D_2}} + J_{\mathrm{perm,HD}} \tag{6}$$

The upstream PC (AB: PC-A, BA: PC-B) which is not connected to the QMS is usually sealed by the valves that are directly attached to the gas inlet and outlet flanges of the OC (AB: V-16 and V-01, BA: V-17 and V-02). However, this implies that during the measurement possible leakages and permeation processes will cause a slow decrease of the initial gas pressure in the upstream PC. For this reason, the presented experimental design offers the possibility to create a gas flow inside of the upstream PC coming from the upstream GMT (AB: GMT-A, BA: GMT-B). The flow enters through the leak valve (AB: V-16, BA: V-17) at the gas inlet of the PC and exits the outlet pipe of the PC before leaving through the downstream leak valve (AB: V-06, BA: V-05) into the RVP-01 via valve V-09. In case the permeation direction BA is used valve V-09 and its pipe connection to the RVP-01 is unplugged from the junction between V-06 and V-08 and connected to the port between the valves V-05 and V-07 (see Fig. 1). To create a homogeneous gas flow which causes a stationary gas pressure in the upstream PC both leak valves should be opened by the same level.

3. Experimental procedures

The presented design of the COOPER experimental set-up allows executing measurements to study different permeation phenomena and to determine material specific hydrogen isotope transport parameters of the sample disk material. For the following description of the experimental procedures permeation direction AB is considered. Before any measurement is executed the entire experimental system is evacuated and degassed until a sufficiently low base pressure is reached. Before gas is injected into the PCs the disk is heated to the desired temperature value and it is waited until thermal equilibrium is attained.

3.1. Mono-isotopic permeation experiment

In a mono-isotopic permeation experiment the permeation of a single hydrogen isotope gas (H_2 or D_2) from a gas filled container through a sample material into vacuum is observed. Such a permeation experiment is usually performed to experimentally obtain the hydrogen isotope permeability [25] or the diffusion coefficient [26] of the sample disk material. Moreover, it permits measuring characteristic surface rate constants that determine the recombination and dissociation velocity of the hydrogen isotopes at the gas-bulk interface [27].

The COOPER experiment is designed for permeation measurements in the *diffusion-limited* and in the *surface-limited* permeation regime. The *diffusion-limited* regime is present at high driving pressures in which the dissociation rate at the gas-metal interface is fast in comparison with the diffusion flux in the bulk material. Permeation measurements in this regime enable the determination of the diffusion coefficient of the sample material by applying the time-lag method [28,29]. It was found that in the *diffusion-limited* regime the steady-state molecular permeation flux J_{perm} through a sample material of thickness d_{SD} is approximately proportional to the square root of the gas pressure $J_{\mathrm{perm}} \approx \Phi\cdot\sqrt{P}/d_{\mathrm{SD}}$ with Φ being the temperature dependent hydrogen isotope permeability of the sample material [30]. By measuring the permeation flux for different temperatures while keeping the pressure constant the temperature relation of the permeability is obtained. The *surface-limited* permeation regime describes a case in which the driving pressure of the gas is low causing the diffusion flux to be large in

comparison with the dissociation rate. In this regime, the molecular permeation flux is approximately proportional to the pressure P and can be expressed by the relation $J_{perm} \approx \frac{1}{2}\sigma K_d P$ where σ is the surface roughness factor [30]. The temperature dependent dissociation coefficient K_d is measured for different temperatures while keeping the pressure constant.

To execute a mono-isotopic permeation measurement with the presented set-up H_2 or D_2 is filled into PC-A and PC-B is evacuated. The permeation flux of the corresponding hydrogen isotope through the SD into PC-B is measured for different upstream pressures and different sample temperatures as described in Section 2.1.

3.2. Multi-isotopic permeation experiment

The COOPER experiment enables deuterium permeation flux measurements by introducing D_2 into the upstream PC while H_2 gas is additionally present in the upstream PC (co-permeation) or in the downstream PC (counter-permeation). The objective of these measurements is the observation of co- and counter-permeation as a permeation mitigation or enhancement mechanism as proposed in previous studies [17,19,20]. The experimental data gained from these experiments will be used for the validation of numerical multi-isotopic transport models [14,16–18,20]. Therefore, experimental data shall be compared with simulation results. With the COOPER experiment special focus is placed on the experimental analysis of the following HCPB relevant co- and counter-permeation scenarios.

3.2.1. Co-permeation experiment

Co-permeation measurements are based on the injection of a $D_2 + H_2$ mixture into PC-A while PC-B is evacuated. The gases co-permeate side by side from PC-A into PC-B. The time evolving deuterium permeation flux is measured via the *open path* as described in Section 2.1 until steady state diffusion occurs. Following an evacuation and degassing of the system this measurement is repeatedly executed for different H_2 pressures ranging from 0Pa to 1×10^5Pa while the D_2 partial pressure is kept constant. It is analysed how an increase of the H_2 partial pressure in PC-A influences the deuterium permeation flux into PC-B.

3.2.2. Counter-permeation experiment

For counter-permeation measurements PC-A is filled with D_2 gas while H_2 is inserted into PC-B. Both gases counter-permeate into the opposite PC. Since PC-B contains a gas pressure in the low vacuum regime the permeating particles are required to enter the QMS system via the *leak path*. The deuterium permeation flux is measured as described in Section 2.2 until steady state permeation establishes. The measurements are repeatedly executed increasing the H_2 partial pressure in PC-B from 0Pa to 1×10^5Pa while the D_2 partial pressure inserted into PC-A remains the same. In this way it is observed under which conditions counter-permeating H_2 gas mitigates or enhances the deuterium permeation flux. After each measurement the PT is evacuated and degassed.

4. Conclusion

Tritium transport simulations suggest that adding H_2 gas to the coolant of an HCPB breeding blanket system could, in certain partial pressure regimes, have a mitigating effect on tritium permeation into the coolant. For the experimental observation of this promising method a new multi-isotopic permeation experiment has been designed within the scope of this work. It is called COOPER experiment and allows investigating the isotopic effect of co- and counter-permeation of different hydrogen isotopes through an EUROFER disk under HCPB relevant conditions. The permeation chamber constitutes two gas cavities inside of a vacuum chamber which are separated by the sample disk. A band heater is clamped around a custom-designed copper ring which surrounds the sample disk in its centre. The heat enters the disk at its circular boundary edge, thus reaching temperatures of up to 600 °C. Finite element thermal calculations anticipate a nearly homogeneous radial temperature profile which would establish inside of the disk in steady state. The vacuum chamber surrounding the permeation tube enables an efficient degassing of the hot permeation cell walls and will significantly lower the contamination of the measurement system with atmospheric gas molecules. For reliable measurement results these are essential requirements. A gas line system consisting of two gas tanks permits the user to mix, pre-heat and inject arbitrary partial pressure configurations of Ar, H_2 and D_2 gas into both permeation cells. Gas pressures of below 1×10^{-1}Pa up to 1×10^5Pa can be well controlled and maintained stable, even at elevated temperatures. The experimental design enables measuring H_2, HD or D_2 permeation fluxes into an evacuated or H_2 filled permeation cell using a calibrated QMS. Therefore, the downstream permeation chamber and the QMS are either directly connected or linked via a manual leak valve. The COOPER experiment has the purpose to validate numerical simulation results of HCPB permeation scenarios and to measure material specific hydrogen transport parameters. Matching experimental and simulation results would confirm a controlled H_2 injection to the coolant as a promising method to mitigate tritium permeation in HCPB breeding blankets.

CRediT authorship contribution statement

S.J. Hendricks: Conceptualization, Methodology, Investigation, Visualization, Writing – original draft. **E. Carella:** Conceptualization, Writing – review & editing, Supervision, Funding acquisition. **D. Jimenez:** Methodology, Supervision. **J.M. Garcia:** Supervision. **J. Molla:** Project administration.

Declaration of Competing Interest

The authors declare that they have no known competing financial interests or personal relationships that could have appeared to influence the work reported in this paper.

Acknowledgments

This work has been carried out within the framework of the EUROfusion Consortium and has received funding from the Euratom research and training programme 2014–2018 and 2019–2020 under grant agreement No 633053. The views and opinions expressed herein do not necessarily reflect those of the European Commission. This work has been partially funded by the MINECO Ministry under project ENE2013-43650-R. S.J. Hendricks acknowledges a pre-PhD contract of the Spanish MICINN.

References

[1] F.A. Hernandez, HCPB Design Report 2015, Final Report for EUROfusion, EFDA_D_2MNBH9, 2016.https://idm.euro-fusion.org/?uid=2MNBH9
[2] F.A. Hernndez, F. Arbeiter, L.V. Boccaccini, E. Bubelis, V. Chakin, I. Cristescu, B. E. Ghidersa, M. Gonzalez, W. Hering, T. Hernandez, X.Z. Jin, M. Kamlah, B. Kiss, R. Knitter, M.H.H. Kolb, P. Kurinskiy, O. Leys, I.A. Maione, M. Moscardini, G. Ndasi, H. Neuberger, P. Pereslavtsev, S. Pupeschi, R. Rolli, S. Ruck, G. A. Spagnuolo, P.V. Vladimirov, C. Zeile, G. Zhou, Overview of the HCPB research activities in EUROfusion, IEEE Trans. Plasma Sci. 46 (2018) 2247–2261, https://doi.org/10.1109/TPS.2018.2830813.
[3] E. Carella, C. Moreno, F.R. Urgorri, D. Demange, J. Castellanos, D. Rapisarda, Tritium behavior in HCPB breeder blanket unit: modeling and experiments, Fusion Sci. Technol. 71 (2017) 357–362, https://doi.org/10.1016/j.fusengdes.2017.01.051.
[4] G. Federici, A.R. Raffray, M.A. Abdou, Mistral: a comprehensive model for tritium transport in lithium-base ceramics: Part II: comparison of model predictions with experimental results, J. Nucl. Mater. 173 (2) (1990) 214–228, https://doi.org/10.1016/0022-3115(90)90258-O.
[5] C. Johnson, Tritium behavior in lithium ceramics, J. Nucl. Mater. 270 (1999) 212–220, https://doi.org/10.1016/S0022-3115(98)00905-2.

[6] T. Kinjyo, M. Nishikawa, Tritium release behavior from Li_4SiO_4, Fusion Sci. Technol. 46 (2004) 561–570, https://doi.org/10.13182/FST04-A591.
[7] E. Carella, C. Moreno, F.R. Urgorri, D. Rapisarda, A. Ibarra, Tritium modelling in HCPB breeder blanket at a system level, Fusion Eng. Des. 124 (2017) 687–691, https://doi.org/10.1016/j.fusengdes.2017.01.051.
[8] F. Cismondi, Solid and Liquid Breeder Blankets [Lecture], Politcnico de Turn, Italy, 2011.https://staff.polito.it/roberto.zanino/sub1/teach.html
[9] A. Aiello, I. Ricapito, G. Benamati, R. Valentini, Hydrogen isotopes permeability in Eurofer 97 martensitic steel, Fusion Sci. Technol. 41 (3P2) (2002) 872–876, https://doi.org/10.13182/FST41-872.
[10] A. Perujo, K. Forcey, Tritium permeation barriers for fusion technology, Fusion Eng. Des. 28 (1995) 252–257, https://doi.org/10.1016/0920-3796(95)90045-4.
[11] K. Kizu, T. Tanabe, Counter-diffusion and counter-permeation of deuterium and hydrogen through palladium, J. Nucl. Mater. 258 (1998) 1133–1137, https://doi.org/10.1016/S0022-3115(98)00393-6.
[12] K. Kizu, T. Tanabe, Deuterium permeation through metals under hydrogen counter flow, J. Nucl. Mater. 266 (1999) 561–565, https://doi.org/10.1016/S0022-3115(98)00589-3.
[13] K. Kizu, A. Pisarev, T. Tanabe, Co-permeation of deuterium and hydrogen through Pd, J. Nucl. Mater. 289 (3) (2001) 291–302, https://doi.org/10.1016/S0022-3115(01)00428-7.
[14] T. Takeda, J. Iwatsuki, Counter-permeation of deuterium and hydrogen through Inconel 600, Nucl. Technol. 146 (2004) 83–95, https://doi.org/10.13182/NT04-A3490.
[15] M. Shimada, R. Pawelko, Tritium permeability measurement in hydrogen-tritium system, Fusion Eng. Des. 129 (2018) 134–139, https://doi.org/10.1016/j.fusengdes.2018.02.033.
[16] H. Zhang, A. Ying, M. Abdou, M. Shimada, B. Pawelko, S. Cho, Characterization of tritium isotopic permeation through ARAA in diffusion limited and surface limited regimes, Fusion Sci. Technol. 72 (3) (2017) 416–425, https://doi.org/10.1080/15361055.2017.1333826.
[17] C. Moreno, F.R. Urgorri, D. Rapisarda, The isotopic effect on tritium permeation in breeding blankets. Invited Speaker Presentation, 12th International Conference on Tritium Science & Technology, 2019.
[18] N. Bidica, I. Cristescu, E. Carcadea, A. Bornea, C. Bucur, N. Sofilca, A. Lazar, Modelling synergistic isotope effects of the permeation of multiple hydrogen isotopes through metals, Fusion Eng. Des. 146 (2019) 1938–1941, https://doi.org/10.1016/j.fusengdes.2019.03.071.
[19] C. Moreno, F.R. Urgorri, A. Rueda, J. Serna, Tritium control strategy in the breeding blanket concepts. Invited Speaker Presentation, SOFT2020, 2020.https://soft2020.eu/Programme/Speakers
[20] E. Carella, S.J. Hendricks, O. Matti, Evaluation of Tritium Permeation in the He Coolant from the HCPB Considering Various Scenarios of Hydrogen Partial Pressures in the Cooling Gas, EFDA_D_2P4A5H, 2020.https://idm.euro-fusion.org/?uid=2P4A5H
[21] N. Bidica, N. Sofilca, G.C. Popescu, B.F. Monea, C.M. Moraru, Experimental setup and pre-experiment issues for multi-component hydrogen isotopes permeation through metals in non-steady-state, Fusion Eng. Des. 157 (2020) 111677, https://doi.org/10.1016/j.fusengdes.2020.111677.
[22] D. Klimenko, F. Arbeiter, V. Pasler, G. Schlindwein, A. von der Weth, K. Zinn, Definition of the Q-PETE experiment for investigation of hydrogen isotopes permeation through the metal structures of a DEMO HCPB breeder zone, Fusion Eng. Des. 136 (2018) 563–568, https://doi.org/10.1016/j.fusengdes.2018.03.024.
[23] S. Davies, J. Rees, D. Seymour, Threshold ionisation mass spectrometry (TIMS); a complementary quantitative technique to conventional mass resolved mass spectrometry, Vacuum 101 (2014) 416–422, https://doi.org/10.1016/j.vacuum.2013.06.004.
[24] W. Umrath, Fundamentals of Vacuum Technology, Leybold Vacuum GmbH, Colone, Germany, 2016.
[25] M. Malo, B. Garcinuno, D. Rapisarda, Experimental refutation of the deuterium permeability in vanadium, niobium and tantalum, Fusion Eng. Des. 146 (2019) 224–227, https://doi.org/10.1016/j.fusengdes.2018.12.025.
[26] S. Xiukui, X. Jian, L. Yiyi, Hydrogen permeation behaviour in austenitic stainless steels, Mater. Sci. Eng. 114 (1989) 179–187, https://doi.org/10.1016/0921-5093(89)90857-5.
[27] E. Serra, A. Perujo, Influence of the surface conditions on permeation in the deuterium MANET system, J. Nucl. Mater. 240 (3) (1997) 215–220, https://doi.org/10.1016/S0022-3115(96)00679-4.
[28] J. Crank, The Mathematics of Diffusion, Oxford University Press, Bristol, England, 1975.
[29] F. Waelbroeck, P. Wienhold, J. Winter, T. Banno, Influence of Bulk and Surface Phenomena on the Hydrogen Permeation through Metals. Technical Report Nr. Juel-1966, Forschungszentrum Jlich GmbH Zentralbibliothek, 1984.http://hdl.handle.net/2128/12413
[30] G.A. Esteban, A. Perujo, L.A. Sedano, B. Mancinelli, The surface rate constants of deuterium in the reduced activating martensitic steel OPTIFER-IVb, J. Nucl. Mater. 282 (2000) 89–96, https://doi.org/10.1016/S0022-3115(00)00485-2.